

Effects of the particle-particle channel on properties of low-lying vibrational states

A. P. Severyukhin,¹ V. V. Voronov,¹ and Nguyen Van Giai²

¹*Bogoliubov Laboratory of Theoretical Physics, Joint Institute for Nuclear Research, RU-141980 Dubna, Moscow region, Russia*

²*Institut de Physique Nucléaire, CNRS-IN2P3, Université Paris-Sud, F-91406 Orsay Cedex, France*

(Received 16 November 2007; published 29 February 2008)

Making use of the finite rank separable approach for the quasiparticle random phase approximation enables one to perform nuclear structure calculations in very large two-quasiparticle spaces. The approach is extended to take into account the residual particle-particle interaction. The calculations are performed by using Skyrme interactions in the particle-hole channel and density-dependent zero-range interactions in the particle-particle channel. To illustrate our approach, we study the properties of the lowest quadrupole states in the even-even nuclei ^{128}Pd , ^{130}Cd , $^{124-134}\text{Sn}$, $^{128-136}\text{Te}$, and ^{136}Xe .

DOI: [10.1103/PhysRevC.77.024322](https://doi.org/10.1103/PhysRevC.77.024322)

PACS number(s): 21.60.Jz, 23.20.-g, 27.60.+j

I. INTRODUCTION

The low-energy spectrum is a key character of excitations of nuclei in the presence of pairing correlations. The new spectroscopic studies of exotic nuclei stimulate a development of the nuclear models [1–3] to describe properties of nuclei away from the stability line. One of the standard tools for nuclear structure studies is the quasiparticle random phase approximation (QRPA) with the self-consistent mean-field derived by making use of effective nucleon-nucleon interactions that are taken whether as nonrelativistic two-body forces [4,5] or derived from relativistic Lagrangians [6]. Because these QRPA calculations are performed with the same energy functional as that determining the mean-field the introduction of new parameters is not required. Such an approach describes the properties of the low-lying states less accurately than more phenomenological ones, but the results are in a reasonable agreement with experimental data [7–11].

When the residual interaction is separable [12], the QRPA equations can be easily solved no matter how many two-quasiparticle configurations are involved. Starting from an effective interaction of the Skyrme type, a finite rank separable approximation was proposed [13] for the particle-hole (p-h) residual interaction. Such an approach allows one to perform structure calculations in very large particle-hole spaces. Thus, the self-consistent mean-field can be calculated within the Hartree-Fock (HF) method with the original Skyrme interactions, whereas the RPA solutions are obtained with the finite rank approximation for the p-h matrix elements. This approach can be extended to include the pairing correlations within the BCS approximation [14]. Alternative schemes to factorize the p-h interaction have also been considered in Refs. [15–17].

Due to the anharmonicity of vibrations there is a coupling between one-phonon and more complex states [2] and the complexity of calculations beyond the standard QRPA increases rapidly with the size of the configuration space. We have generalized our approach to take into account a coupling between the one- and two-phonon components of wave functions in Ref. [18], where we follow the basic ideas of the quasiparticle-phonon model (QPM) [12]. However, the single-quasiparticle spectrum and the parameters of the

residual interaction are calculated with Skyrme forces. Note that the QPM [12] can achieve very detailed predictions for nuclei away from closed shells [19], but it is difficult to extrapolate the phenomenological parameters of the model Hamiltonian to new regions of nuclei.

In the present work, we propose an extension of our approach by taking into account the particle-particle (p-p) residual interaction. As an application we present the evolution of lowest quadrupole states in even-even nuclei around the ^{132}Sn region. Using the neutron-rich radioactive ion beams, the recent $B(E2)$ measurements through Coulomb excitation in inverse kinematics give an opportunity to compare our results and the experimental data [20,21].

This article is organized as follows: in Sec. II we sketch our method, where the residual interaction is obtained by the finite rank approximation. The Hamiltonian is constructed in Sec. II A whereas detailed expressions for the residual interaction are given in Appendixes A and B. We consider the QRPA equations in the case of separable residual interactions in Sec. II B, and the solving of these equations is explained in Appendix C. In Sec. III we show how this approach can be applied to treat the low-lying states. Results of calculations for characteristics of the 2_1^+ states in the Sn and Te isotopes and the $N = 82$ isotones are discussed in Sec. IV. Conclusions are drawn in Sec. V.

II. METHOD OF CALCULATION

A. The model Hamiltonian

The starting point of the method is the HF-BCS calculation [3] of the ground states. We restrict the present discussion to the case of spherical symmetry. The continuous part of the single-particle spectrum is discretized by diagonalizing the HF Hamiltonian on a harmonic oscillator basis [22]. We work in the quasiparticle representation defined by the canonical Bogoliubov transformation

$$a_{jm}^+ = u_j \alpha_{jm}^+ + (-1)^{j-m} v_j \alpha_{j-m}, \quad (1)$$

where jm denote the quantum numbers $nljm$. We use the Skyrme interaction [23] in the p-h channel, while the pairing

correlations are generated by a surface peaked density-dependent zero-range force

$$V_{\text{pair}}(\mathbf{r}_1, \mathbf{r}_2) = V_0 \left(1 - \frac{\rho(r_1)}{\rho_c}\right) \delta(\mathbf{r}_1 - \mathbf{r}_2). \quad (2)$$

In definition (2), $\rho(r_1)$ is the particle density in coordinate space, ρ_c is equal to the nuclear saturation density, and the strength V_0 is a parameter fixed to reproduce the odd-even mass difference of nuclei in the studied region. In Sec. III, we discuss how to make the choice of the parameter V_0 . To avoid divergences, it is necessary to introduce a cutoff in the single-particle space. This cutoff limits the active pairing space above the Fermi level. As proposed in Refs. [24,25], we have used the smooth cutoff by multiplying the p-p matrix elements with cutoff factors η_j taken as

$$\eta_j^2 = \left(1 + \exp\left(\frac{E_j - \lambda - \Delta E}{\mu}\right)\right)^{-1}. \quad (3)$$

E_j are the single-particle energies, and $\lambda_{n,p}$ is the chemical potential. In our calculations we have set the energy cutoff ΔE equal to 10 MeV above the Fermi level, the width parameter μ being 0.5 MeV.

The residual interaction $V_{\text{res}}^{\text{ph}}$ in the p-h channel and $V_{\text{res}}^{\text{pp}}$ in the p-p channel can be obtained as the second derivatives of the energy density functional with respect to the particle density ρ and the pair density $\tilde{\rho}$, respectively. Following the method introduced in Ref. [13] we simplify $V_{\text{res}}^{\text{ph}}$ by approximating it by its Landau-Migdal form. For Skyrme interactions the Landau parameters are functions of the coordinate \mathbf{r} and all parameters with $l > 1$ vanish. We keep only the $l = 0$ terms in $V_{\text{res}}^{\text{ph}}$ and the expressions for F_0^{ph} , G_0^{ph} , F_0^{pp} , and G_0^{pp} in terms of the Skyrme force parameters can be found in Ref. [26]. In this work we study only normal parity states and one can neglect the spin-spin terms because they play a minor role. The Coulomb and spin-orbit residual interactions are also dropped. Therefore we can write the residual interaction in the following form:

$$V_{\text{res}}^a(\mathbf{r}_1, \mathbf{r}_2) = N_0^{-1} [F_0^a(r_1) + F_0^a(r_1)\tau_1 \cdot \tau_2] \delta(\mathbf{r}_1 - \mathbf{r}_2), \quad (4)$$

where a is the channel index $a = \{\text{ph}, \text{pp}\}$, τ_i is the isospin operator, and $N_0 = 2k_F m^* / \pi^2 \hbar^2$, with k_F and m^* standing for the Fermi momentum and nucleon effective mass. For the p-p channel the expressions for F_0^{pp} and G_0^{pp} have the following forms:

$$F_0^{\text{pp}}(r) = \frac{1}{4} N_0 V_0 \left(1 - \frac{\rho(r)}{\rho_c}\right), \quad (5)$$

$$G_0^{\text{pp}}(r) = F_0^{\text{pp}}(r). \quad (6)$$

As a matter of fact, the definition of the pairing force (2) involves the energy cutoff of the single-particle space to restrict the active pairing space within the mean-field approximation. This energy cutoff is still required to eliminate the p-p matrix elements of the residual interaction in the case of the subshells that are far from the Fermi level. The region of influence of the residual p-p interaction is confined to the BCS subspace

$$V_{1234}^{\text{pp}} = \tilde{V}_{1234}^{\text{pp}} \eta_1 \eta_2 \eta_3 \eta_4, \quad (7)$$

where all subshells below the energy cutoff are included.

The two-body matrix elements

$$V_{1234} = \int \phi_1^*(\mathbf{r}_1) \phi_2^*(\mathbf{r}_2) V_{\text{res}}(\mathbf{r}_1, \mathbf{r}_2) \phi_3(\mathbf{r}_1) \phi_4(\mathbf{r}_2) d\mathbf{r}_1 d\mathbf{r}_2 \quad (8)$$

can be written as

$$\begin{aligned} V_{j_1 m_1 j_2 m_2 j_3 m_3 j_4 m_4}^{\text{ph}} &= \hat{J}^{-2} \sum_{JM} (-1)^{j-M+j_3-m_3+j_4-m_4} \\ &\times \langle j_1 m_1 j_3 - m_3 | J - M \rangle \langle j_2 m_2 j_4 - m_4 | JM \rangle \\ &\times \langle j_1 || i^J Y_J || j_3 \rangle \langle j_2 || i^J Y_J || j_4 \rangle I^{\text{ph}}(j_1 j_2 j_3 j_4), \quad (9) \\ V_{j_1 m_1 j_2 m_2 j_3 m_3 j_4 m_4}^{\text{pp}} &= \sum_{JM} \langle j_1 m_1 j_2 m_2 | JM \rangle \langle j_3 m_3 j_4 m_4 | JM \rangle \\ &\times \eta_{j_1} \eta_{j_2} \eta_{j_3} \eta_{j_4} \sum_{\lambda} \left\{ \begin{matrix} j_4 & j_3 & J \\ j_1 & j_2 & \lambda \end{matrix} \right\} \\ &\times (-1)^{j_2+j_3+\lambda+J} \langle j_1 || i^\lambda Y_\lambda || j_3 \rangle \\ &\times \langle j_2 || i^\lambda Y_\lambda || j_4 \rangle I^{\text{pp}}(j_1 j_2 j_3 j_4) \quad (10) \end{aligned}$$

in the p-h and p-p channels, respectively. In the above expressions, $\hat{J} = \sqrt{2J+1}$, $\langle j_1 || i^J Y_J || j_3 \rangle$ is the reduced matrix element of the spherical harmonics $Y_{J\mu}$ [27], $I^a(j_1 j_2 j_3 j_4)$ is the radial integral:

$$\begin{aligned} I^a(j_1 j_2 j_3 j_4) &= N_0^{-1} \int_0^\infty (F_0^a(r) + F_0^a(r)\tau_1 \cdot \tau_2) \\ &\times u_{j_1}(r) u_{j_2}(r) u_{j_3}(r) u_{j_4}(r) \frac{dr}{r^2}, \quad (11) \end{aligned}$$

where the radial wave functions $u(r)$ are related to the single-particle wave functions,

$$\phi_{i,m}(1) = \frac{u_i(r_1)}{r_1} \mathcal{Y}_{l_i, j_i}^m(\hat{r}_1, \sigma_1). \quad (12)$$

We see that the p-h matrix elements are in the separable form in the angular coordinates. The separability of the antisymmetrized p-p matrix elements is proved in Appendix A. The radial integrals (11) can be calculated accurately by choosing a large enough cutoff radius R and using an N -point integration Gauss formula with abscissas r_k and weights w_k . Thus, the residual interaction can be reduced to a finite rank separable form:

$$\begin{aligned} \hat{V}_{\text{res}} &= \frac{1}{4} \sum_a \sum_{1234} (V_{1234}^a - V_{1243}^a) : a_1^\dagger a_2^\dagger a_4 a_3 : \\ &= -\frac{1}{2} \sum_{a\lambda\mu} \sum_{k=1}^N \sum_{\tau q=\pm 1} (\kappa_0^{(a,k)} + q\kappa_1^{(a,k)}) \\ &\times : \hat{M}_{\lambda\mu}^{(a,k)+}(\tau) \hat{M}_{\lambda\mu}^{(a,k)}(q\tau) : . \quad (13) \end{aligned}$$

We sum over the proton (p) and neutron (n) indexes and the notation $\{\tau = (n, p)\}$ is used. A change $\tau \leftrightarrow -\tau$ means a change $p \leftrightarrow n$. $\kappa^{(\text{ph},k)}$ ($\kappa^{\text{pp},k}$) are the multipole interaction strengths in the p-h (p-p) channel and they can be

expressed as

$$\begin{pmatrix} \kappa_0^{(\text{ph},k)} \\ \kappa_1^{(\text{ph},k)} \\ \kappa_0^{(\text{pp},k)} \\ \kappa_1^{(\text{pp},k)} \end{pmatrix} = -N_0^{-1} \frac{Rw_k}{2r_k^2} \begin{pmatrix} F_0^{\text{ph}}(r_k) \\ F_0^{\text{pp}}(r_k) \\ \frac{1}{2} F_0^{\text{pp}}(r_k) \\ \frac{1}{2} F_0^{\text{pp}}(r_k) \end{pmatrix}. \quad (14)$$

The multipole operators entering the normal products in Eq. (13) are defined as follows:

$$\hat{M}_{\lambda\mu}^{(\text{ph},k)+}(\tau) = \hat{\lambda}^{-1} \sum_{jj'mm'}^{\tau} (-1)^{j+m} \langle jmj' - m' | \lambda\mu \rangle f_{jj'}^{(\lambda,k)} a_{jm}^+ a_{j'm'}, \quad (15)$$

$$\hat{M}_{\lambda\mu}^{(\text{pp},k)+}(\tau) = (-1)^{\lambda-\mu} \hat{\lambda}^{-1} \sum_{jj'mm'}^{\tau} \langle jmj'm' | \lambda\mu \rangle f_{jj'}^{(\lambda,k)} \eta_j \eta_{j'} a_{jm}^+ a_{j'm'}, \quad (16)$$

where $f_{j_1 j_2}^{(\lambda,k)}$ are the single-particle matrix elements of the multipole operators,

$$f_{j_1 j_2}^{(\lambda,k)} = u_{j_1}(r_k) u_{j_2}(r_k) \langle j_1 || i^\lambda Y_\lambda || j_2 \rangle. \quad (17)$$

Technical details of the proof of Eq. (13) for particle-hole channel are given in Appendix B.

The residual interaction (13) is represented in terms of bi-fermion quasiparticle operators and their conjugates:

$$B(jj'; \lambda\mu) = \sum_{mm'} (-1)^{j'+m'} \langle jmj'm' | \lambda\mu \rangle \alpha_{jm}^+ \alpha_{j'-m'}, \quad (18)$$

$$A^+(jj'; \lambda\mu) = \sum_{mm'} \langle jmj'm' | \lambda\mu \rangle \alpha_{jm}^+ \alpha_{j'm'}. \quad (19)$$

Thus, the Hamiltonian of our method has the same form as the Hamiltonian of the QPM [12], but the single-quasiparticle spectrum and the parameters of the residual interaction are calculated with the Skyrme forces.

B. QRPA equations for separable residual interactions

We introduce the phonon creation operators

$$Q_{\lambda\mu i}^+ = \frac{1}{2} \sum_{jj'} (X_{jj'}^{\lambda i} A^+(jj'; \lambda\mu) - (-1)^{\lambda-\mu} Y_{jj'}^{\lambda i} A(jj'; \lambda - \mu)), \quad (20)$$

where the index λ denotes total angular momentum and μ is its z projection in the laboratory system. One assumes that the ground state is the QRPA phonon vacuum $|0\rangle$. We define the excited states as $Q_{\lambda\mu i}^+ |0\rangle$ with the normalization condition

$$\langle 0 | [Q_{\lambda\mu i}, Q_{\lambda\mu i'}^+] | 0 \rangle = \delta_{ii'}. \quad (21)$$

Making use of the linearized equation-of-motion approach [1] one can get the QRPA equations [3]

$$\begin{pmatrix} \mathcal{A} & \mathcal{B} \\ -\mathcal{B} & -\mathcal{A} \end{pmatrix} \begin{pmatrix} X \\ Y \end{pmatrix} = \omega \begin{pmatrix} X \\ Y \end{pmatrix}, \quad (22)$$

where the $\mathcal{A}_{(j_1 j_1')(j_2 j_2')}^{(\lambda)}$ matrix is related to forward-going graphs and the $\mathcal{B}_{(j_1 j_1')(j_2 j_2')}^{(\lambda)}$ matrix is related to backward-going graphs. The dimension of the matrices \mathcal{A}, \mathcal{B} is the space size of the two-quasiparticle configurations. In our case, we obtain

$$\begin{aligned} \mathcal{A}_{(j_1 \geq j_1')\tau(j_2 \geq j_2')q\tau}^{(\lambda)} &= \varepsilon_{j_1 j_1'} \delta_{j_2 j_1} \delta_{j_2' j_1'} \delta_{q1} - \hat{\lambda}^{-2} (1 + \delta_{j_2 j_2'})^{-1} \\ &\times \sum_{k=1}^N f_{j_1 j_1'}^{(\lambda,k)} f_{j_2 j_2'}^{(\lambda,k)} [(\kappa_0^{(\text{ph},k)} + q\kappa_1^{(\text{ph},k)}) \\ &\times u_{j_1 j_1'}^{(+)} u_{j_2 j_2'}^{(+)} + (\kappa_0^{(\text{pp},k)} + q\kappa_1^{(\text{pp},k)}) \\ &\times \eta_{j_1 j_1'} \eta_{j_2 j_2'} (v_{j_1 j_1'}^{(+)} v_{j_2 j_2'}^{(+)} + v_{j_1 j_1'}^{(-)} v_{j_2 j_2'}^{(-)})], \end{aligned} \quad (23)$$

$$\begin{aligned} \mathcal{B}_{(j_1 \geq j_1')\tau(j_2 \geq j_2')q\tau}^{(\lambda)} &= -\hat{\lambda}^{-2} (1 + \delta_{j_2 j_2'})^{-1} \\ &\times \sum_{k=1}^N f_{j_1 j_1'}^{(\lambda,k)} f_{j_2 j_2'}^{(\lambda,k)} [(\kappa_0^{(\text{ph},k)} + q\kappa_1^{(\text{ph},k)}) \\ &\times u_{j_1 j_1'}^{(+)} u_{j_2 j_2'}^{(+)} - (\kappa_0^{(\text{pp},k)} + q\kappa_1^{(\text{pp},k)}) \\ &\times \eta_{j_1 j_1'} \eta_{j_2 j_2'} (v_{j_1 j_1'}^{(+)} v_{j_2 j_2'}^{(+)} - v_{j_1 j_1'}^{(-)} v_{j_2 j_2'}^{(-)})], \end{aligned} \quad (24)$$

where $\varepsilon_{jj'} = \varepsilon_j + \varepsilon_{j'}$, $\eta_{jj'} = \eta_j + \eta_{j'}$, $u_{jj'}^{(+)} = u_j v_{j'} + v_j u_{j'}$, and $v_{jj'}^{(\pm)} = u_j u_{j'} \pm v_j v_{j'}$. The explicit solution of the corresponding QRPA equations is given in Appendix C. Thus, this approach enables one to reduce remarkably the dimensions of the matrices that must be inverted to perform structure calculations in very large configuration spaces. It is shown that the matrix dimensions never exceed $6N \times 6N$ independently of the configuration space size. If we omit the residual interaction in the p-p channel then the matrix dimension is reduced by a factor 3 [13,14].

III. DETAILS OF CALCULATIONS

We apply our approach to study characteristics of the lowest vibrational states in the nuclei around the ^{132}Sn region. In this work we use the parametrization SLy4 [23] of the Skyrme interaction. One peculiarity is that the parameters of the force have been adjusted to describe the pure neutron matter. It follows that this parametrization is a good candidate to describe isotopic properties of nuclei from the β -stability line to the neutron drip line. In our calculations the single-particle continuum is discretized [22] by diagonalizing the HF Hamiltonian on a basis of 12 harmonic oscillator shells and cutting off the single-particle spectra at the energy of 100 MeV. This is sufficient to exhaust practically all the energy-weighted sum rule within the QRPA. We use the isospin-invariant surface-peaked pairing force (2). The value $\rho_c = 0.16 \text{ fm}^{-3}$ is the nuclear saturation density for the SLy4 force. The pairing strength V_0 is fitted to reproduce the pairing energies given by

$$P_N = \frac{1}{2}(B(N, Z) + B(N-2, Z) - 2B(N-1, Z)) \quad (25)$$

for neutrons, and similarly for protons. The strength V_0 is taken equal to -940 MeV fm^3 to get a reasonable description

TABLE I. Properties of the 2_1^+ state in ^{130}Te as an illustrative example to demonstrate the effect of the residual p-p interaction.

Residual interaction	E (MeV)	$B(E2 \uparrow)(e^2 \text{fm}^4)$
ph	1.49	3400
ph+pp	1.15	4000
ph+pp (cutoff)	1.27	3600

of the energies (25) for both protons and neutrons. The Landau parameters $F_0^{\text{ph}}, F_0^{\text{ph}'}, G_0^{\text{ph}},$ and $G_0^{\text{ph}'}$ expressed in terms of the Skyrme force parameters [26] depend on k_F . As it is pointed out in our previous works [13,14] one needs to adopt some effective value for k_F to give an accurate representation of the original p-h Skyrme interaction. For the present calculations we use the nuclear matter value for k_F . Our previous investigations [14,18] enable us to conclude that $N = 45$ for the rank of our separable approximation is enough for multiplicities $\lambda \leq 6$ in nuclei with $A \leq 208$. For example, the calculation with $N = 60$ changes results of energies and transition probabilities by no more than 1%.

It is worth mentioning the significance of the energy cutoff of the single-particle space to confine the active space of the residual p-p interaction. Our choice for the cutoff eliminates matrix elements (10) coupling single-particle states inside and outside of the BCS subspace. As can be seen from Table I, omitting the energy cutoff would lead to an overestimation of the effect of the residual p-p interaction on the 2_1^+ energy and $B(E2 \uparrow)$ in ^{130}Te , for example.

IV. RESULTS

A. Sn isotopes

As the first application of the method we investigate the p-p channel effects on energies and transition probabilities of 2_1^+ states in $^{124-134}\text{Sn}$. Results of our calculations for the 2_1^+ energies and $B(E2)$ transition probabilities are compared with experimental data [20,21,28] in Fig. 1. As can be seen from Fig. 1, there is a remarkable increase of the 2_1^+ energy and $B(E2 \uparrow)$ in ^{132}Sn in comparison with those in $^{130,134}\text{Sn}$. As it was explained in our previous paper [18] such a behavior of $B(E2 \uparrow)$ is related with the proportion between the QRPA amplitudes for neutrons and protons in Sn isotopes. Including the p-p channel changes contributions of the main configurations only slightly, but the general structure of the 2_1^+ remains the same. The neutron amplitudes are dominant in all Sn isotopes and the contribution of the main neutron configuration $\{1h_{11/2}, 1h_{11/2}\}$ increases from 58% (61% in the case of the inclusion the p-h interaction only) in ^{124}Sn to 85.6% (85.3% for the p-h case) in ^{130}Sn when neutrons fill the subshell $1h_{11/2}$. At the same time the contribution of the main proton configuration $\{2d_{5/2}, 1g_{9/2}\}$ is decreasing from 15% in ^{124}Sn to 7% in ^{130}Sn . The closure of the neutron subshell $1h_{11/2}$ in ^{132}Sn leads to the vanishing of the neutron pairing. The energy of the first neutron two-quasiparticle pole $\{2f_{7/2}, 1h_{11/2}\}$ in ^{132}Sn is larger than energies of the first poles in $^{130,134}\text{Sn}$

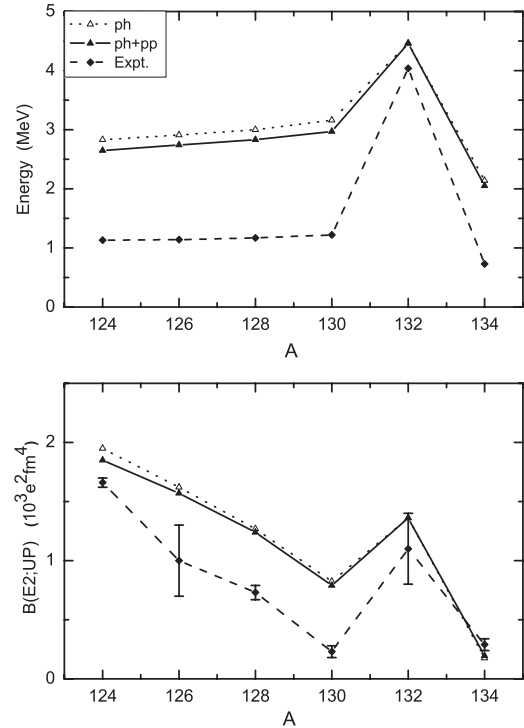


FIG. 1. Energies and $B(E2)$ values for up-transitions to the first 2_1^+ states in $^{124-134}\text{Sn}$.

and the contribution of the $\{2f_{7/2}, 1h_{11/2}\}$ configuration in the doubly magic ^{132}Sn is about 61%. Furthermore, the first pole in ^{132}Sn is closer to the proton poles. This means that the contribution of the proton two-quasiparticle configurations is larger than those in the neighboring isotopes and as a result the main proton configuration $\{2d_{5/2}, 1g_{9/2}\}$ in ^{132}Sn exhausts about 33%. In ^{134}Sn the leading contribution (about 96%) comes from the neutron configuration $\{2f_{7/2}, 2f_{7/2}\}$ and as consequently the $B(E2)$ value is reduced. Such a behavior of the 2_1^+ energies and $B(E2)$ values in the neutron-rich Sn isotopes reflects the shell structure in this region. As one can see from Fig. 1 the inclusion of the p-p channel results in a reduction of energies and transition probabilities. The calculations reproduce very well a general behavior for energies and transition probabilities, but there is some overestimation in comparison with the experimental data. One can expect an improvement if the coupling with the two-phonon components of the wave functions [18] is taken into account. Such calculations are now in progress. It is worth mentioning that the first prediction of the anomalous behavior of 2_1^+ excitations around ^{132}Sn based on the QRPA calculations with a separable quadrupole-plus-pairing Hamiltonian has been done in Ref. [29].

Other QRPA calculations with Skyrme [10,30] and Gogny [31] forces give similar tendencies for the energies and the transition probabilities of 2_1^+ states in $^{124-134}\text{Sn}$. Let us compare our results with the ones in Ref. [30]. In both cases, the same effective interactions, the Skyrme SLy4 [23] in the particle-hole channel and the density-dependent zero-range force (2) in the particle-particle channel, are used. For ^{132}Sn , $E = 5.13$ MeV and $B(E2 \uparrow) = 1370$ e²fm⁴ are represented

in Ref. [30]. Our calculated $B(E2)$ value is in good agreement but our 2_1^+ energy is somewhat smaller. This discrepancy may be related with an approximate treatment of the velocity-dependent terms of Skyrme interactions in our approach. The calculation [30] does not employ this approximation. One can see agreement between the results for the doubly magic ^{132}Sn , but there is a disagreement for the open-shell nuclei. The 2_1^+ energies and $B(E2)$ values are larger in our calculation than those in Ref. [30]. The origin of that cannot be expected to be unique. A possible source of this discrepancy can be the choice of the strength V_0 of the pairing force (2). We fix the V_0 to reproduce the neutron pairing energies (25) for $^{124-134}\text{Sn}$, $^{128-136}\text{Te}$, and ^{136}Xe and the proton pairing energies for $^{128-136}\text{Te}$ and ^{136}Xe . If the pairing strength is fitted to describe the Sn isotopes pairing energies only, then our 2_1^+ energies (for example, see Ref. [18]) are in reasonable agreement with the results [30]. However, the $B(E2)$ values are in worse agreement than the excitation energy. A possible reason is a treatment of velocity-dependent terms of the residual interaction (4) in our method. Besides, in both cases the single-particle continuum is treated approximately. The different schemes of the discretization of the continuum are used in our calculation and in Ref. [30], where the HF Hamiltonian is diagonalized in the coordinate space with the box boundary condition. It is worth mentioning that the $B(E2)$ values are very sensitive to the details of calculations.

B. Te isotopes

Let us now discuss the Te isotopes. The calculated 2_1^+ state energies and transition probabilities $B(E2)$ in the $^{128-136}\text{Te}$ isotopes and experimental data [20,21,28] are shown in Fig. 2.

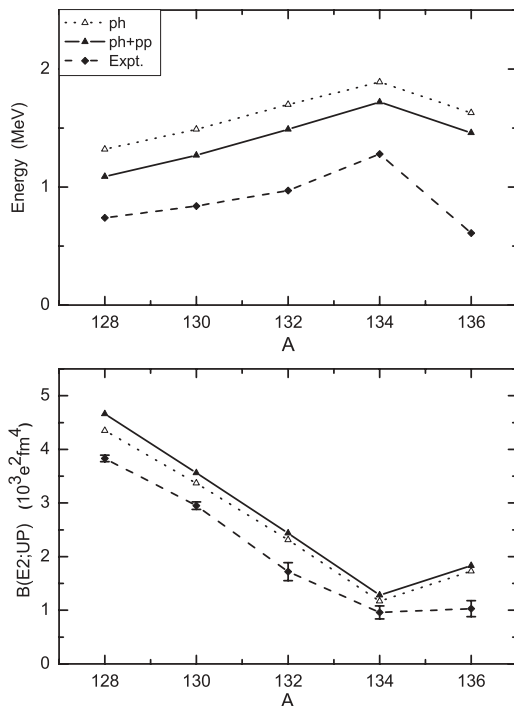


FIG. 2. Energies and $B(E2)$ values for up-transitions to the first 2_1^+ states in $^{128-136}\text{Te}$.

The general behavior of energies of the Te isotopes is similar to that of the Sn isotopes. They have a maximal value at $N = 82$, but the behavior of the $B(E2)$ values is different and corresponds to a standard evolution of the $B(E2)$ near closed shells. As can be seen from Fig. 2, there is a decrease of the 2_1^+ energies due to the inclusion of the p-p channel. At the same time the $B(E2)$ values do not change practically. It means that the collectivity of the 2_1^+ states is reduced. The neutron configurations exhaust about 17 and 28% of the wave function normalization in ^{132}Te and ^{136}Te , respectively. In ^{134}Te the contribution of the neutron configurations is less than 3% and the dominant proton configuration $\{1g_{7/2}, 1g_{7/2}\}$ gives a contribution of about 65% that is almost twice larger than that in the neighboring Te isotopes. As far as a contribution of this configuration into the transition probability is less than contributions of other proton configurations, the $B(E2)$ values have such a behavior near $N = 82$. The structure of the 2_1^+ in ^{132}Te is similar to that in ^{136}Te and as a result the $B(E2)$ values differ slightly.

Our calculations describe correctly the isotopic dependence of energies and transition probabilities and they are in a reasonable agreement with the available experimental data. It is worth mentioning that the anharmonicity effects are strong for the light Te isotopes and the QRPA is not very good in such a case. The $B(E2)$ value in the neutron-rich isotope ^{136}Te is only slightly larger than that of ^{134}Te , in contrast to the trend of Ce, Ba, and Xe isotopes [20,21,28]. As is shown in Ref. [29], such a behavior of $B(E2)$ is related with the shell structure in this region and an interplay between the QRPA amplitudes for neutrons and protons in Te isotopes. The difference in the neutron pairing gaps of $^{132,136}\text{Te}$ plays the key role in

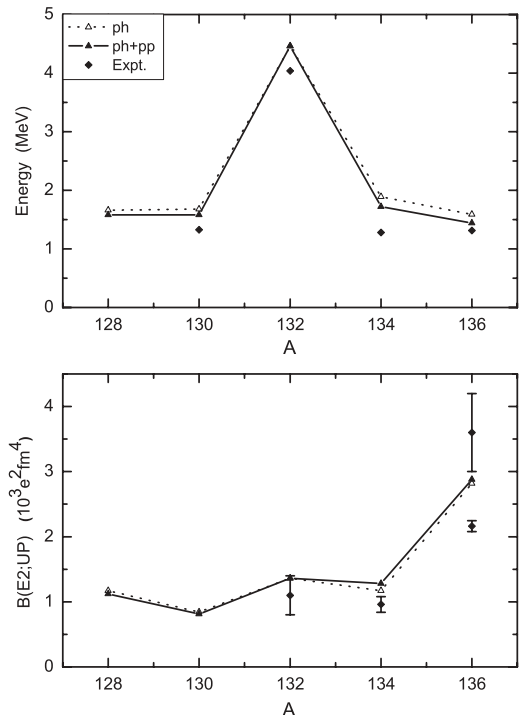


FIG. 3. Energies and $B(E2)$ values for up-transitions to the first 2_1^+ states in the $N = 82$ isotones.

TABLE II. $(M_n/M_p)/(N/Z)$ ratios for the first 2_1^+ states.

Nucleus	^{128}Pd	^{130}Cd	^{132}Sn	^{134}Te	^{136}Xe
Theory	0.47	0.49	0.81	0.54	0.55

explaining this peculiarity. Our calculations give the similar asymmetry around $N = 82$; the average neutron pairing gap is equal to 1.1 MeV for ^{132}Te and 0.9 MeV for ^{136}Te . As a result, it is shown above that the contribution of neutron configurations in ^{132}Te is less than that of those in ^{136}Te .

C. $N = 82$ isotones

It is interesting to study a change of the structure of the 2_1^+ states along the $N = 82$ isotones chain. The $N = 82$ isotones below the doubly magic nucleus ^{132}Sn are crucial for stellar nucleosynthesis [32]. Results of our calculations and existing experimental data [21,28,32,33] are shown in Fig. 3. It can be seen that the inclusion of the p-p channel does not change energies and transition probabilities along this chain. Going along the $N = 82$ isotones chain one can find that 2_1^+ states in ^{128}Pd and ^{130}Cd have a noncollective structure with a domination of the proton configuration $\{1g_{9/2}, 1g_{9/2}\}$. In ^{132}Sn , as is discussed above, the main configurations are the neutron $\{2f_{7/2}, 1h_{11/2}\}$ (61%) and the proton $\{2d_{5/2}, 1g_{9/2}\}$ (33%) ones. In ^{134}Te and ^{136}Xe the 2_1^+ states are very collective and many proton configurations contribute in their structure. The structure peculiarities are reflected in the $B(E2)$ behavior in this chain. Higher collectivity results in an increase of the transition probability. Additional information about the structure of the first 2^+ states can be extracted from the proton scattering experiments (for example, see Ref. [34]) by looking at the ratio of the multipole transition matrix elements M_n/M_p that depends on the relative contributions of the proton and neutron configurations. Results of our calculations are given in Table II, where the M_n/M_p ratio for ^{128}Pd , ^{130}Cd is less than half of N/Z value, indicating a very strong proton contribution. According to our calculations there is a sharp increase of M_n/M_p at $Z = 50$, $N = 82$. Such a behavior of the multipole transition matrix elements M_n/M_p in other nuclei can indicate a shell closure.

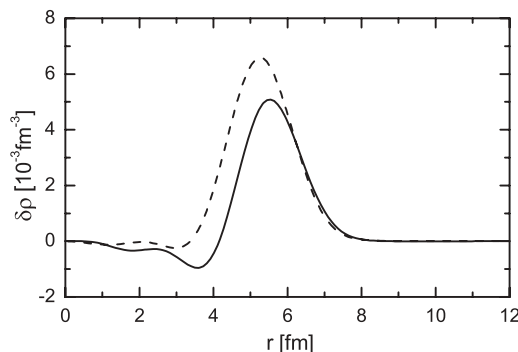


FIG. 4. Neutron (solid line) and proton (dashed line) transition densities of the 2_1^+ state of ^{130}Cd .

Another quantity that characterizes the 2_1^+ state is the transition density. As an example the neutron and proton transition densities of the 2_1^+ state of ^{130}Cd are displayed in Fig. 4. The neutron transition density is shifted outward as compared to the proton transition density due to the presence of the neutron skin. We get a similar tendency in the case of the other isotones but this effect becomes weak in ^{136}Xe .

V. CONCLUSIONS

A finite rank separable approximation for the QRPA calculations with Skyrme interactions that was proposed in our previous work is extended to take into account the residual particle-particle interaction. This approximation enables one to reduce considerably the dimensions of the matrices that must be inverted to perform structure calculations in very large configuration spaces. As an illustration of the method we have studied the energies and transition probabilities of the 2_1^+ states around the ^{132}Sn region. Using the same set of parameters we describe available experimental data and give predictions for the $N = 82$ isotones that are important for stellar nucleosynthesis. Including the quadrupole p-p interaction results in a reduction of the collectivity and this may be more important for nuclei far from closed shells. Such calculations that take into account the two-phonon terms in wave functions are in progress now.

ACKNOWLEDGMENTS

We are grateful to Professor Ch. Stoyanov for valuable discussions. A.P.S. and V.V.V. thank the hospitality of IPN-Orsay where a part of this work was done. This work was partly supported by the IN2P3-JINR agreement.

APPENDIX A

In this appendix, we derive the formulas that help us to represent the antisymmetrized p-p matrix elements in the separable form in the angular coordinates.

In Eq. (10) the sum over λ can be transformed into

$$\begin{aligned}
& \sum_{\lambda} (-1)^{j_2+j_3+J+\lambda} \begin{Bmatrix} j_4 & j_3 & J \\ j_1 & j_2 & \lambda \end{Bmatrix} \langle j_1 \| i^{\lambda} Y_{\lambda} \| j_3 \rangle \langle j_2 \| i^{\lambda} Y_{\lambda} \| j_4 \rangle \\
& = \hat{j}_1 \hat{j}_2 \hat{j}_3 \hat{j}_4 (16\pi)^{-1} i^{l_3+l_4-l_1-l_2} \\
& \times \left((1 + (-1)^{l_1+l_2+l_3+l_4}) \begin{pmatrix} j_3 & j_4 & J \\ -\frac{1}{2} & -\frac{1}{2} & 1 \end{pmatrix} \right. \\
& \times \left. \begin{pmatrix} j_1 & j_2 & J \\ -\frac{1}{2} & -\frac{1}{2} & 1 \end{pmatrix} - ((-1)^{l_1+l_3} + (-1)^{l_2+l_4}) (-1)^{j_1+j_3} \right. \\
& \times \left. \left. \begin{pmatrix} j_3 & J & j_4 \\ -\frac{1}{2} & 0 & \frac{1}{2} \end{pmatrix} \begin{pmatrix} j_1 & J & j_2 \\ -\frac{1}{2} & 0 & \frac{1}{2} \end{pmatrix} \right) \right). \tag{A1}
\end{aligned}$$

Then, the antisymmetrized p-p matrix elements take the form

$$V_{1234}^{\text{pp}} - V_{1243}^{\text{pp}} = \hat{f}^{-2} \sum_{JM} \langle j_1 m_1 j_2 m_2 | JM \rangle \times \langle j_3 m_3 j_4 m_4 | JM \rangle \langle j_1 || i^J Y_J || j_2 \rangle \langle j_3 || i^J Y_J || j_4 \rangle \times I^{\text{pp}}(j_1 j_2 j_3 j_4) \eta_{j_1} \eta_{j_2} \eta_{j_3} \eta_{j_4}. \quad (\text{A2})$$

APPENDIX B

For the sake of completeness we consider how to get the finite rank separable form (13) for the p-h residual interaction (4). In Eq. (9) the p-h matrix elements are written as the sum of the term represented in the separable form in the angular coordinates. Using an N -point integration Gauss formula, the nonseparable radial term (11) is replaced by the separable ansatz. Thus we can get the direct terms in the following separable form:

$$\begin{aligned} & \frac{1}{2} \sum_{1234} V_{1234}^{\text{ph}} : a_1^+ a_2^+ a_4 a_3 : \\ &= -\frac{1}{2} \sum_{\lambda\mu} \sum_{k=1}^N \sum_{\tau q=\pm 1} (\kappa_0^{(\text{ph},k)} + q\kappa_1^{(\text{ph},k)}) \\ & \quad \times : \hat{M}_{\lambda\mu}^{(\text{ph},k)+}(\tau) \hat{M}_{\lambda\mu}^{(\text{ph},k)}(q\tau) :. \end{aligned} \quad (\text{B1})$$

To change 3 \leftrightarrow 4 indexes in Eq. (9) the exchange terms can be expressed as the sum of compositions of the $\hat{M}^+ \hat{M}$ operators:

$$\begin{aligned} & \frac{1}{2} \sum_{1234} V_{1243}^{\text{ph}} : a_1^+ a_2^+ a_4 a_3 : \\ &= \frac{1}{2} \sum_{\lambda\mu} \sum_{k=1}^N \sum_{\tau q=\pm 1} (\kappa_0^{(\text{ph},k)} + q\kappa_1^{(\text{ph},k)}) \\ & \quad \times : \hat{M}_{\lambda\mu}^{(\text{ph},k)+}(\tau) \hat{M}_{\lambda\mu}^{(\text{ph},k)}(q\tau) :. \end{aligned} \quad (\text{B2})$$

APPENDIX C

Taking into account the residual p-p interaction we show how the finite rank separable form of the residual force (13) can simplify the solution of the QRPA equations (22). In the $6N$ -dimensional space we introduce a vector

$$\begin{pmatrix} D_0(\tau) \\ D_+(\tau) \\ D_-(\tau) \end{pmatrix}$$

by its components

$$D_{\beta}^k(\tau) = \begin{pmatrix} D_{\beta}^k(\tau) \\ D_{\beta}^k(-\tau) \end{pmatrix}, \quad \beta = \{0, +, -\}$$

$$\begin{aligned} D_0^{\lambda ik}(\tau) &= \sum_{jj'}^{\tau} f_{jj'}^{(\lambda k)} u_{jj'}^{(+)} (X_{jj'}^{\lambda i} + Y_{jj'}^{\lambda i}), \\ D_{\pm}^{\lambda ik}(\tau) &= \sum_{jj'} f_{jj'}^{(\lambda k)} \eta_{jj'} v_{jj'}^{(\pm)} (X_{jj'}^{\lambda i} \mp Y_{jj'}^{\lambda i}) \end{aligned} \quad (\text{C1})$$

The index k runs over the N -dimensional space ($k = 1, 2, \dots, N$). Following our previous paper [14] the QRPA equations (22) can be reduced to the following set of equations:

$$\begin{pmatrix} \mathcal{M}_{00}(\tau) - 1 & \mathcal{M}_{0+}(\tau) & \mathcal{M}_{0-}(\tau) \\ \mathcal{M}_{+0}(\tau) & \mathcal{M}_{++}(\tau) - 1 & \mathcal{M}_{+-}(\tau) \\ \mathcal{M}_{-0}(\tau) & \mathcal{M}_{-+}(\tau) & \mathcal{M}_{--}(\tau) - 1 \end{pmatrix} \times \begin{pmatrix} D_0(\tau) \\ D_+(\tau) \\ D_-(\tau) \end{pmatrix} = 0, \quad (\text{C2})$$

where \mathcal{M} is the $2N \times 2N$ matrix

$$\mathcal{M}_{\beta\beta'}^{kk'}(\tau) = \begin{pmatrix} (\kappa_0^{(\beta',k')} + \kappa_1^{(\beta',k')}) T_{\beta\beta'}^{kk'}(\tau) & (\kappa_0^{(\beta',k')} - \kappa_1^{(\beta',k')}) T_{\beta\beta'}^{kk'}(\tau) \\ (\kappa_0^{(\beta',k')} - \kappa_1^{(\beta',k')}) T_{\beta\beta'}^{kk'}(-\tau) & (\kappa_0^{(\beta',k')} + \kappa_1^{(\beta',k')}) T_{\beta\beta'}^{kk'}(-\tau) \end{pmatrix}, \quad 1 \leq k, \quad k' \leq N. \quad (\text{C3})$$

In the definition (C3), $\kappa^{(0,k')} = \kappa^{(\text{ph},k')}$, $\kappa^{(\pm,k')} = \kappa^{(\text{pp},k')}$. The matrix elements $T^{kk'}$ have the following form:

$$\begin{aligned} T_{00}^{kk'}(\tau) &= \sum_{jj'}^{\tau} \chi_{jj'}^{\lambda kk'} (u_{jj'}^{(+)})^2 \varepsilon_{jj'}, \\ T_{++}^{kk'}(\tau) &= \sum_{jj'}^{\tau} \chi_{jj'}^{\lambda kk'} (v_{jj'}^{(+)} \eta_{jj'})^2 \varepsilon_{jj'}, \\ T_{--}^{kk'}(\tau) &= \sum_{jj'}^{\tau} \chi_{jj'}^{\lambda kk'} (v_{jj'}^{(-)} \eta_{jj'})^2 \varepsilon_{jj'}, \\ T_{0+}^{kk'}(\tau) &= T_{+0}^{kk'}(\tau) = \sum_{jj'}^{\tau} \chi_{jj'}^{\lambda kk'} u_{jj'}^{(+)} v_{jj'}^{(+)} \eta_{jj'} \omega_{\lambda i}, \end{aligned}$$

$$\begin{aligned} T_{0-}^{kk'}(\tau) &= T_{-0}^{kk'}(\tau) = \sum_{jj'}^{\tau} \chi_{jj'}^{\lambda kk'} u_{jj'}^{(+)} v_{jj'}^{(-)} \eta_{jj'} \varepsilon_{jj'}, \\ T_{+-}^{kk'}(\tau) &= T_{-+}^{kk'}(\tau) = \sum_{jj'}^{\tau} \chi_{jj'}^{\lambda kk'} v_{jj'}^{(+)} v_{jj'}^{(-)} (\eta_{jj'})^2 \omega_{\lambda i}, \end{aligned}$$

where

$$\chi_{jj'}^{\lambda kk'} = \frac{f_{jj'}^{(\lambda k)} f_{jj'}^{(\lambda k')}}{\hat{\lambda}^2 (\varepsilon_{jj'}^2 - \omega_{\lambda i}^2)}.$$

One can see that the matrix dimensions never exceed $6N \times 6N$ independently of the size of the two-quasiparticle configuration. The excitation energies $\omega_{\lambda i}$ are the roots of the secular

equation

$$\det \begin{pmatrix} \mathcal{M}_{00}(\tau) - 1 & \mathcal{M}_{0+}(\tau) & \mathcal{M}_{0-}(\tau) \\ \mathcal{M}_{+0}(\tau) & \mathcal{M}_{++}(\tau) - 1 & \mathcal{M}_{+-}(\tau) \\ \mathcal{M}_{-0}(\tau) & \mathcal{M}_{-+}(\tau) & \mathcal{M}_{--}(\tau) - 1 \end{pmatrix} = 0. \quad (\text{C4})$$

The phonon amplitudes corresponding to the QRPA eigenvalue $\omega_{\lambda i}$ are obtained by Eq. (22) and the normalization condition (21).

-
- [1] D. J. Rowe, *Nuclear Collective Motion, Models and Theory* (Methuen, London, 1970).
- [2] A. Bohr and B. Mottelson, *Nuclear Structure* (Benjamin, New York, 1975), Vol. 2.
- [3] P. Ring and P. Schuck, *The Nuclear Many Body Problem* (Springer, Berlin, 1980).
- [4] D. Vautherin and D. M. Brink, *Phys. Rev. C* **5**, 626 (1972).
- [5] D. Gogny, *Nuclear Self-consistent Fields*, edited by G. Ripka and M. Porneuf (North-Holland, Amsterdam, 1975).
- [6] P. Ring, *Prog. Part. Nucl. Phys.* **37**, 193 (1996), and references cited therein.
- [7] E. Khan, N. Sandulescu, M. Grasso, and Nguyen Van Giai, *Phys. Rev. C* **66**, 024309 (2002).
- [8] S. Péru, J. F. Berger, and P. F. Bortignon, *Eur. Phys. J. A* **26**, 25 (2005).
- [9] D. Vretenar, A. V. Afanasjev, G. A. Lalazissis, and P. Ring, *Phys. Rep.* **409**, 101 (2005).
- [10] J. Terasaki and J. Engel, *Phys. Rev. C* **74**, 044301 (2006).
- [11] N. Paar, D. Vretenar, E. Khan, and G. Colò, *Rep. Prog. Phys.* **70**, 691 (2007).
- [12] V. G. Soloviev, *Theory of Atomic Nuclei: Quasiparticles and Phonons* (Institute of Physics, Bristol and Philadelphia, 1992).
- [13] Nguyen Van Giai, Ch. Stoyanov, and V. V. Voronov, *Phys. Rev. C* **57**, 1204 (1998).
- [14] A. P. Severyukhin, Ch. Stoyanov, V. V. Voronov, and Nguyen Van Giai, *Phys. Rev. C* **66**, 034304 (2002).
- [15] T. Suzuki and H. Sagawa, *Prog. Theor. Phys.* **65**, 565 (1981).
- [16] P. Sarriguren, E. Moya de Guerra, and A. Escuderos, *Nucl. Phys.* **A658**, 13 (1999).
- [17] V. O. Nesterenko, J. Kvasil, and P.-G. Reinhard, *Phys. Rev. C* **66**, 044307 (2002).
- [18] A. P. Severyukhin, V. V. Voronov, and Nguyen Van Giai, *Eur. Phys. J. A* **22**, 397 (2004).
- [19] S. Galès, Ch. Stoyanov, and A. I. Vdovin, *Phys. Rep.* **166**, 125 (1988).
- [20] D. C. Radford *et al.*, *Phys. Rev. Lett.* **88**, 222501 (2002).
- [21] D. C. Radford *et al.*, *Nucl. Phys.* **A752**, 264c (2005).
- [22] J. P. Blaizot and D. Gogny, *Nucl. Phys.* **A284**, 429 (1977).
- [23] E. Chabanat, P. Bonche, P. Haensel, J. Meyer, and R. Schaeffer, *Nucl. Phys.* **A635**, 231 (1998); **A643**, 441(E) (1998).
- [24] S. J. Krieger *et al.*, *Nucl. Phys.* **A517**, 275 (1990).
- [25] P. Bonche, H. Flocard, P.-H. Heenen, S. Krieger, and M. S. Weiss, *Nucl. Phys.* **A443**, 39 (1985).
- [26] Nguyen Van Giai and H. Sagawa, *Phys. Lett.* **B106**, 379 (1981).
- [27] K. L. G. Heyde, *The Nuclear Shell Model* (Springer-Verlag, Berlin, 1994).
- [28] S. Raman, C. W. Nestor, Jr., and P. Tikkanen, *At. Data Nucl. Data Tables* **78**, 1 (2001).
- [29] J. Terasaki, J. Engel, W. Nazarewicz, and M. Stoitsov, *Phys. Rev. C* **66**, 054313 (2002).
- [30] G. Colò, P. F. Bortignon, D. Sarchi, D. T. Khoa, E. Khan, and Nguyen Van Giai, *Nucl. Phys.* **A722**, 111c (2003).
- [31] G. Giambrone *et al.*, *Nucl. Phys.* **A726**, 3 (2003).
- [32] A. Jungclaus *et al.*, *Phys. Rev. Lett.* **99**, 132501 (2007).
- [33] G. Jakob *et al.*, *Phys. Rev. C* **65**, 024316 (2002).
- [34] J. K. Jewel *et al.*, *Phys. Lett.* **B454**, 181 (1999).